

Design and biological evaluation of phenyl imidazole analogs as hedgehog signaling pathway inhibitors

Chiyu Sun¹  | Ying Zhang² | Han Wang¹ | Zhengxu Yin¹ | Lingqiong Wu¹ | Yanmiao Huang¹ | Wenhui Zhang¹ | Youbing Wang¹ | Qibo Hu¹

¹School of Pharmacy, Shenyang Medical College, Shenyang, China

²School of Chemical Engineering, Shenyang University of Chemical Technology, Shenyang, China

Correspondence

Chiyu Sun, School of Pharmacy, Shenyang Medical College, Shenyang 110034, China.
Email: scy_dream@126.com

Funding information

the Science and Technology Fund Project of Shenyang Medical College, Grant/Award Number: 20191027; Liaoning Science and Technology Project Management, Grant/Award Number: 20170520026

Abstract

The hedgehog (Hh) signaling pathway is involved in diverse aspects of cellular events. Aberrant activation of Hh signaling pathway drives oncogenic transformation for a wide range of cancers, and it is therefore a promising target in cancer therapy. In the principle of association and ring-opening, we designed and synthesized a series of Hh signaling pathway inhibitors with phenyl imidazole scaffold, which were biologically evaluated in Gli-Luc reporter assay. Compound **25** was identified to possess high potency with nanomolar IC₅₀, and moreover, it preserved the inhibition against wild-type and drug-resistant Smo-overexpressing cells. A molecular modeling study of compound **25** expounded its binding mode to Smo receptor, providing a basis for the further structural modification of phenyl imidazole analogs.

KEYWORDS

hedgehog signaling, inhibitors, modeling, phenyl imidazole, Smo receptor

1 | INTRODUCTION

The Hedgehog(Hh)signaling pathway is not only associated with the maintenance and repair of many human tissues, but also plays an important role in cell growth, survival, and metastasis (Galperin et al., 2019; Makley & Gestwicki, 2013; Owens et al., 2017; Sharpe et al., 2015). Hh signaling is silent in normal cells, and however, its abnormal activation is associated with basal cell carcinoma (BCC), medulloblastoma (MB), pancreatic cancer, acute myeloid leukemia (AML), colon, and prostate cancer (Berman et al., 2002; Cortes et al., 2019; DeBerardinis et al., 2014; Domenech et al., 2012; Mathew et al., 2014; Vesci et al., 2018). Aberrant Hh signaling is mainly driven by either ligand-dependent or Patched (Ptch) mutation mechanism and induces Ptch to release smoothed (Smo) protein, promoting the translocation of its downstream Gli protein into the nucleus to express Hh target gene (Mas & Altaba, 2010; Salaritabar et al., 2019; Trinh et al., 2014; Wahid et al., 2016). Undoubtedly, there is an increasing level of interests in modulating the Hh signaling pathway for cancer treatment.

Smo is the most studied Hh pathway component as a drug target, and its inhibition leads to down-regulation of those genes associated with cancer growth and progression. Most Hh pathway inhibitors suppress the function of Smo receptor. To date, Vismodegib (**1**), Sonidegib (**2**) and Glasdegib (**3**) have been the Smo antagonists approved by the U.S. Food and Drug Administration (FDA) for the treatment of BCC and AML (Angelaud et al., 2016; Lindsley, 2016; Munchhof et al., 2012; Pan et al., 2010; Robarge et al., 2009; Sheridan, 2019) (Figure 1). Despite the significant accomplishment in the development of Hh pathway inhibitors, the clinical use of **1** and **2** is severely restricted by virtue of their several adverse effects including diarrhea, taste disturbance, hair loss, and muscle spasms (Ghirga et al., 2018). Alternatively, acquired resistance to these drugs has become a major barrier for their continued advancement (Prichard et al., 2015). For instance, Smo D473H mutation was discovered from metastatic BCC and MB patient with relapse after treatment with **1** (Dijkgraaf et al., 2011; Yauch et al., 2009). Smo D477G, a comparable murine Smo mutant, in the mouse

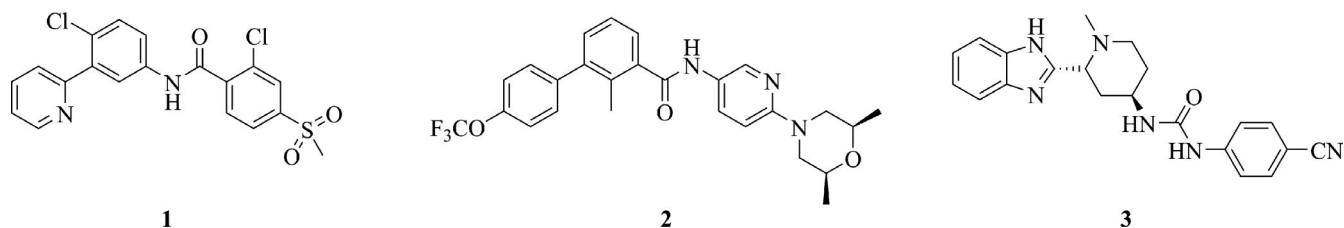


FIGURE 1 Representative structures of Smo inhibitors

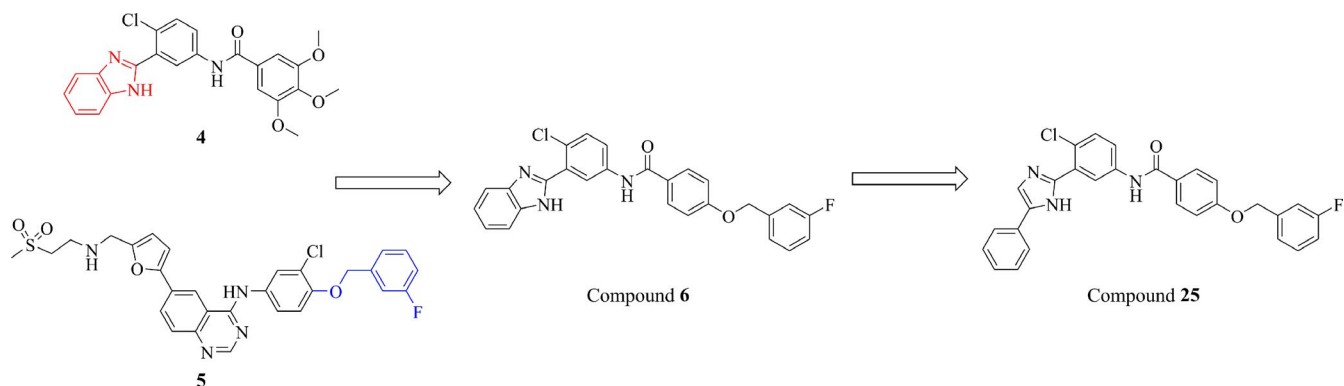
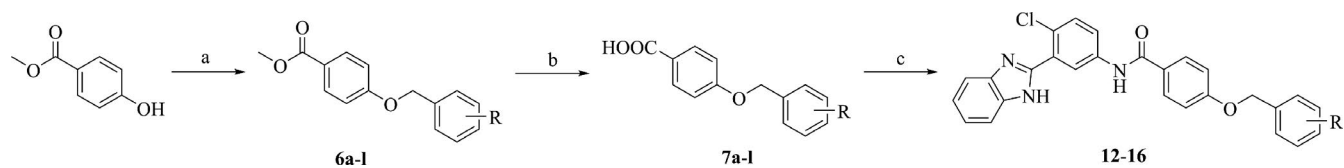
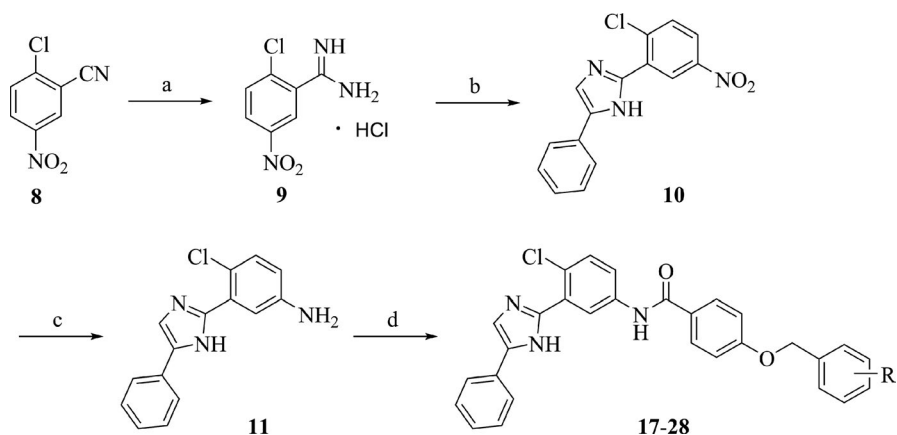


FIGURE 2 Design strategy of novel phenyl imidazole derivatives [Colour figure can be viewed at wileyonlinelibrary.com]



SCHEME 1 (a) substituted benzyl bromide, K_2CO_3 , acetone, $80^\circ C$, 5 hr; (b) NaOH, aqueous alcohol, $75^\circ C$, reflux, 2 hr; (c) (i) $(COCl)_2$, pyridine cat.; (ii) 3-(1H-benzodimidazol-2-yl)-4-chloroaniline, Et_3N , CH_2Cl_2 , rt, 12 hr

SCHEME 2 (a) (i) CH_3ONa , CH_3OH , $-15^\circ C$, 2h; NH_4Cl , $40^\circ C$, 3 hr, (ii) 2-bromoacetophenone, $NaHCO_3$, THF, reflux, $40^\circ C$, 20 hr; (c) $SnCl_2 \cdot 2H_2O$, ethanol, HCl, $80^\circ C$, reflux, 8 hr; (d) HATU, DIPEA, CH_2Cl_2 , **7a-1**, rt, overnight



MB model was drug-resistant as well (Coni et al., 2013). Albeit Smo mutation has no effect on Hh signal transduction, it diminished the affinity of ligands to Smo receptor and disrupted their binding. This finding highlights the continued efforts and interests in research and development of novel chemotype Hh pathway inhibitors.

In the past decade, some benzimidazole analogs as potential Hh inhibitors have been discovered by the high-throughput

screening campaign, for instance, compound **3**, HhAntag691 and SANT-2 (Bariwal et al., 2019). HhAntag691 has been early reported by Curis and Genentech as a potent Hh inhibitor with low nanomolar affinity for Smo (Romer et al., 2004). SANT-2 is a known Smo antagonist with an IC_{50} of 98 nM in the Shh light II assay (Chen et al., 2002). Later, lead optimization of SANT-2 identified TC132 (**4**) with an IC_{50} value of 80 nM, slightly more potent than SANT-2. Büttner

TABLE 1 Hh signaling pathway inhibition of designed compounds

Compound 12-16		Compound 17-28			
Compound	R	Gli-luc reporter IC ₅₀ ^a (μM)	Compound	R	Gli-luc reporter IC ₅₀ ^a (μM)
12	4-CF ₃	1.86 ± 0.17	22	4-F	0.43 ± 0.05
13	2-Cl	1.30 ± 0.06	23	3-CF ₃	0.02 ± 0.01
14	2,4-Cl ₂	0.98 ± 0.08	24	2-F	0.04 ± 0.02
15	4-Me	0.75 ± 0.12	25	3-F	0.01 ± 0.01
16	2-F	0.17 ± 0.05	26	2,4-Cl ₂	0.09 ± 0.02
17	-	1.37 ± 0.11	27	4-Me	0.12 ± 0.07
18	4-CF ₃	0.62 ± 0.06	28	3-Cl	1.16 ± 0.05
19	2-Cl	0.41 ± 0.03	4 ^b	-	0.09 ± 0.01
20	2,3-Cl ₂	0.06 ± 0.02	1 ^c	-	0.02 ± 0.01
21	3,4-Cl ₂	0.29 ± 0.08			

^aResults expressed as the mean ± standard deviation of three separate IC₅₀ determinations. For each determination, concentration–inhibition curves were acquired in triplicate and then averaged to afford a single IC₅₀ curve with a 95% confidence interval.

^bUsed as a lead compound.

^cUsed as a positive control.

et al reported that exchange of benzimidazole core in compound 4 with other heterocyclic rings, such as indole, benzothiazole, and benzoxazole, led to decrease in activity (Büttner et al., 2009). Therefore, benzimidazole is an efficacious moiety for Hh inhibition. In addition, the benzyloxy group was regarded as a bioactive structure normally found in antineoplastic agent like lapatinib (5) (Petrov et al., 2006). In our effort to probe novel Hh pathway inhibitors, we introduced benzyloxy moiety into compound 4 to replace the metabolically labile trimethoxy groups (Figure 2). Encouragingly, this modification led to compound 6 with enhanced anti-Hh activity as measured in Gli-Luc reporter assay (IC₅₀ of 0.07 μM as comparison to 0.09 μM for compound 4). In an attempt to further pursue the chemical structural space, replacement of benzimidazole with phenyl imidazole moiety obtained compound 25 according to ring-opening strategy. The emergence of a rotatable bond between phenyl and imidazole was able to reduce its rigidity, which was expected to improve Smo-binding affinity. The recent determination of Smo-vismodegib crystal structures (PDB code 5L7I) allowed us to examine the interaction patterns between the ligands and Smo receptor (Byrne et al., 2016). The predicted Smo-binding affinity of compound 25 was superior to compound 4, because their docking score was −11.65 and −8.49 kcal/mol, respectively. In this study, a series of phenyl imidazole

derivatives were prepared, and their evaluation on Hh signaling pathway inhibition was reported.

2 | RESULTS AND DISCUSSION

The synthetic routes for the target compounds were outlined in Schemes 1, 2. Methylparaben was etherified with substituted benzyl bromide in acetone to afford compounds 6a–l, which was hydrolyzed to the key intermediates 7a–l in refluxing ethanol for 2 hr. The intermediate

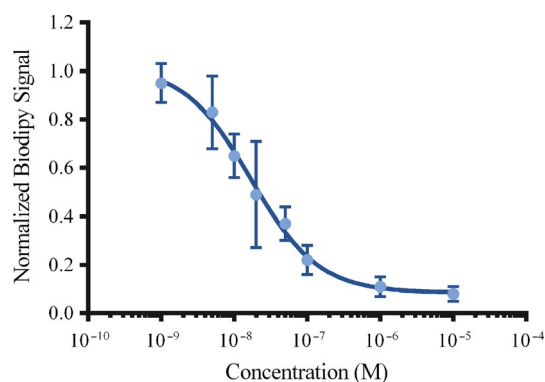


FIGURE 3 In vitro inhibition of Smo for compound 25. The values are an average of triplicate separate determinations [Colour figure can be viewed at wileyonlinelibrary.com]

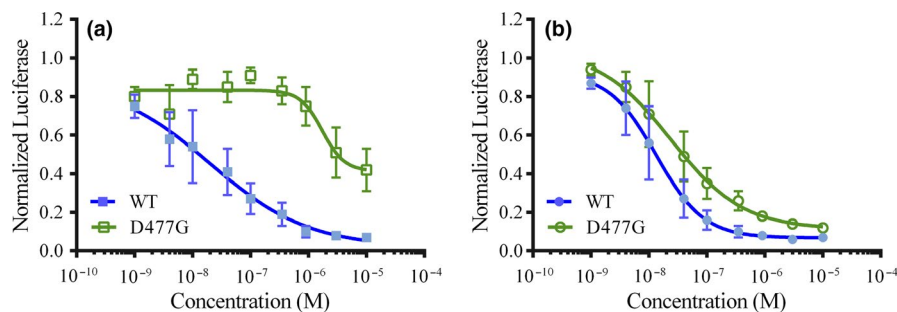


FIGURE 4 The inhibition of drug-resistant Smo mutant for compound **25**. The inhibition of Gli-Luc reporter activity by vismodegib (a) and compound **25** (b) in NIH3T3-Gli-Luc cells overexpressing wild-type Smo or Smo D477G. Error bars represent standard deviation of three parallel groups ($n = 3$) [Colour figure can be viewed at wileyonlinelibrary.com]

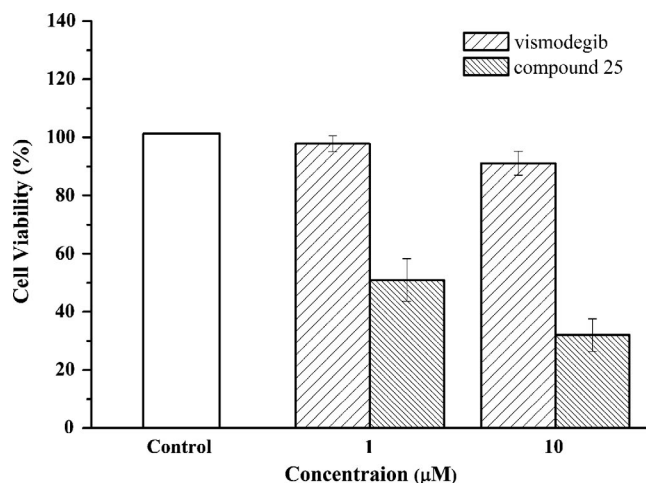


FIGURE 5 Cell viability of DAOY cells treated with the indicated doses of vismodegib and compound **25** for 48 hr. Data represent the average of three independent experiments

3-(1H-benzo[d]imidazol-2-yl)-4-chloroaniline was synthesized in accordance with the reported procedure (Büttner et al., 2009), before its amidation with **7a–I** gave the target compounds **12–16**. 2-chloro-5-nitrobenzotrile reacted with sodium methylate and ammonium chloride in alkaline conditions to form amidine hydrochloride **9**. Then, the intermediate **10** was obtained via condensation of **9** and 2-bromoacetophenone. **10** and stannous chloride refluxed in acidic ethanol solution, and its reduction product was intermediate **11**. Finally, **11** reacted with **7a–I** to give the target compound **17–28**.

The target compound involved the following three regions: A, B, and a linker. Region A contained benzimidazole moiety and phenyl imidazole moiety. Region B involved benzyloxyphenyl group. The amide bond was the linker. The inhibitory activity of compound **12–28** on Hh signaling pathway was evaluated by Gli-Luc reporter kit. Compound **1** was positive control, and compound **4** was lead compound. The results expressed as half maximal inhibitory concentration (IC_{50}) values and were presented in Table 1. Initially, region A in the tested compounds was focused. Delightedly,

the phenyl imidazole derivatives exhibited more potency as compared with the benzimidazole counterparts (**12** vs. **18**, **13** vs. **19**, **14** vs. **26**, **15** vs. **27**, and **16** vs. **24**), indicating that ring-opening structural modification enhanced their Hh inhibition. Further investigations were performed to study the effect of different substituents on the phenyl ring (region B) on Hh inhibition. The introduction of fluoro atom (**22**) or methyl (**27**) in the para-position was superior to trifluoromethyl surrogate (**18**). Ortho-fluoro (**24**) derivative exhibited improved potency than ortho-chlorine analog (**19**). Besides, meta-fluoro derivative (**25**, $IC_{50} = 0.01 \mu\text{M}$) displayed higher activity as compared to other electron-withdrawing groups such as meta-trifluoromethyl (**23**, $IC_{50} = 0.02 \mu\text{M}$) and meta-chlorine (**28**, $IC_{50} = 1.16 \mu\text{M}$). Moreover, the anti-Hh activity of fluoro atom in the meta-position (**25**) was stronger as compared to that in ortho- (**24**, $IC_{50} = 0.04 \mu\text{M}$) or para-position (**22**, $IC_{50} = 0.43 \mu\text{M}$). Although double chlorine substituents (**20**, **21**, and **26**) were effective against Hh signaling, they were inferior in potencies to **25**. Compared with **4**, four of the target compounds (**20**, **23**, **24**, and **25**) showed higher potency with IC_{50} values $< 0.06 \mu\text{M}$. Compound **25** was identified as the most potent compound in this study. More importantly, the potency of compound **25** was twofold higher as compared to **1**, suggesting that it was a promising Hh pathway inhibitor.

The Hh inhibitory activities of this series of compounds probably attributed to their interaction with Smo, since compound **25** effectively competed with BODIPY-cyclopamine in CHO-K1 cells overexpressing wild-type (WT) Smo, with IC_{50} values of 17 nM (Figure 3). Next, it was hypothesized that **25** might be active against the drug-resistant Smo mutant, and therefore, we over-expressed both WT mouse Smo and its mutant D477G with GFP in the NIH3T3-Gli-Luc reporter cell line. Consistent with previous reports, mutation of Smo can confer resistance to **1**. As presented in Figure 4, compound **1** suppressed WT Smo-overexpressing cells with an IC_{50} of 20 nM, and however, its inhibition of mutant Smo-overexpressing cells declined sharply. On the contrary, compound **25** inhibited WT and mutant Smo-overexpressing cells with similar potencies ($IC_{50} = 14 \text{ nM}$ for WT, $IC_{50} = 25 \text{ nM}$ for

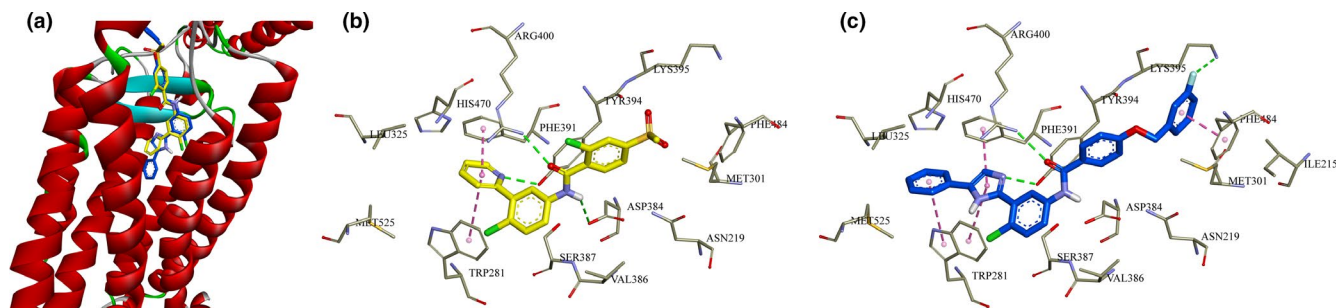


FIGURE 6 (a) Overlay of compound **25** (blue) and original ligand vismodegib (yellow) in binding pocket of Smo. (b) Docking conformation of vismodegib (yellow) at the binding site. (c) Docking conformation of compound **25** (blue) at the binding site. Hydrogen bonds are represented by the dashed green lines. The dashed pink lines represent π - π interaction. Surrounding amino acid is shown in gray stick format and labeled [Colour figure can be viewed at wileyonlinelibrary.com]

mutant). The twofold shift in IC_{50} indicated that the D477G mutation did not significantly interfere with the binding of **25** to Smo. Next, the cytotoxicity assay on Hh-driven cancer cells was performed (Figure 5). DAOY cell lines were a suitable human MB model with constitutive Hh activation, which was reported to be resistant to **1** in vitro. Although **1** was less active against DAOY cells, compound **25** apparently decreased proliferation and survival of DAOY cells. Moreover, the cell viabilities of **25** were 51% and 32% at concentrations of 1 and 10 μ M, respectively.

To further elucidate the binding mode of this series of compounds with Smo receptor, a detailed molecular docking study was performed. The predicted binding affinity of compound **25** was the most among all, with the docking score of -11.65 kcal/mol (Table S1). As shown in Figure 6a, compound **1** (yellow) bound in the pocket closer to the upper opening of Smo, and the binding orientations of compound **1** and **25** (blue) superimposed well with each other. In the binding mode (Figure 6b,c), these two compounds shared similar hydrogen bond with Arg400 to amide bond, and Tyr394 shared to nitrogen atom of pyridine or imidazole. In accordance with pyridine ring on **1**, imidazole ring on **25** allowed π - π interaction with Phe391 and Trp281. These common interactions suggested the importance of imidazole ring and amide bond in region A and linker. Differently, the fluorine on **25** formed a hydrogen bond with Lys395. The phenyl rings in region A and B formed π - π interaction with Trp281 and Phe484. Similar results were observed in the conformations of other compounds (Figure S1). The computational modeling study explained the preferable Hh inhibition of compound **25** at the molecular level.

3 | CONCLUSION

In summary, a series of structural modified phenyl imidazole analogs were designed on the basis of pharmacological association and ring-opening strategy. The synthesized compounds were evaluated in Gli-luciferase assay, and

compounds **20**, **23**, **24**, and **25** exhibited more potent activity than the lead compound TC132. In particular, compound **25** showed the highest Hh inhibitory potency with an IC_{50} value of 0.01 μ M, which was twofold higher than the launched drug vismodegib. Our preliminary investigation indicated that meta-fluoro benzyloxy group was well tolerated for enhancement of activity in the target compounds. Additionally, both wild-type and mutant Smo were effectively suppressed by **25**, and it displayed moderate antiproliferation against DAOY cells in vitro. Computational simulations offered the molecular basis for rationalizing Hh inhibition of the phenyl imidazole derivatives. Further studies on the structural optimization of these derivatives are currently underway in our laboratory.

ACKNOWLEDGMENTS

This work was supported financially by Liaoning Science and Technology Project Management (grant number 20170520026); the Science and Technology Fund Project of Shenyang Medical College (grant numbers 20191027).

CONFLICT OF INTEREST

The authors report no conflict of interest.

ORCID

Chiyu Sun  <https://orcid.org/0000-0001-5736-4022>

REFERENCES

- Angelaud, R., Reynolds, M., Venkatramani, C., Savage, S., Trafelet, H., Landmesser, T., Demel, P., Levis, M., Ruha, O., Rueckert, B., & Jaeggi, H. (2016). Manufacturing development and genotoxic impurity control strategy of the hedgehog pathway inhibitor vismodegib. *Organic Process Research & Development*, *20*, 1509–1519. <https://doi.org/10.1021/acs.oprd.6b00208>
- Bariwal, J., Kumar, V., Dong, Y. X., & Mahato, R. I. (2019). Design of hedgehog pathway inhibitors for cancer treatment. *Medicinal Research Reviews*, *39*, 1137–1204. <https://doi.org/10.1002/med.21555>
- Berman, D. M., Karhadkar, S. S., Hallahan, A. R., Pritchard, J. I., Eberhart, C. G., Watkins, D. N., Chen, J. K., Cooper, M. K., Taipale,

- J., Olson, J. M., & Beachy, P. A. (2002). Medulloblastoma growth inhibition by hedgehog pathway blockade. *Science*, 297, 1559–1561. <https://doi.org/10.1126/science.1073733>
- Büttner, A., Seifert, K., Cottin, T., Sarli, V., Tzagkaroulaki, L., Scholz, S., & Giannis, A. (2009). Synthesis and biological evaluation of SANT-2 and analogues as inhibitors of the hedgehog signaling pathway. *Bioorganic & Medicinal Chemistry*, 17, 4943–4954. <https://doi.org/10.1016/j.bmc.2009.06.008>
- Byrne, E. F., Sircar, R., Miller, P. S., Hedger, G., Luchetti, G., Nachtergaele, S., Tully, M. D., Mydock-McGrane, L., Covey, D. F., Rambo, R. P., Sansom, M. S., Newstead, S., Rohatgi, R., & Siebold, C. (2016). Structural basis of smoothed regulation by its extracellular domains. *Nature*, 535, 517–522. <https://doi.org/10.1038/nature18934>
- Chen, J. K., Taipale, J., Young, K. E., Maiti, T., & Beachy, P. A. (2002). Small molecule modulation of smoothed activity. *Proceedings of the National Academy of Sciences USA*, 99, 14071–14076. <https://doi.org/10.1073/pnas.182542899>
- Coni, S., Infante, P., & Gulino, A. (2013). Control of stem cells and cancer stem cells by hedgehog signaling: Pharmacologic clues from pathway dissection. *Biochemical Pharmacology*, 85, 623–628. <https://doi.org/10.1016/j.bcp.2012.11.001>
- Cortes, J. E., Gutzmer, R., Kieran, M. W., & Solomon, J. A. (2019). Hedgehog signaling inhibitors in solid and hematological cancers. *Cancer Treatment Reviews*, 76, 41–50. <https://doi.org/10.1016/j.ctrv.2019.04.005>
- DeBerardinis, A. M., Madden, D. J., Banerjee, U., Sail, V., Raccuia, D. S., DeCarlo, D., Lemieux, S. M., Meares, A., & Hadden, M. K. (2014). Structure-activity relationships for vitamin d3-based aromatic a-ring analogues as hedgehog pathway inhibitors. *Journal of Medicinal Chemistry*, 57, 3724–3736. <https://doi.org/10.1021/jm401812d>
- Dijkgraaf, G. J. P., Alicka, B., Weinmann, L., Januario, T., West, K., Modrusan, Z., Burdick, D., Goldsmith, R., Robarge, K., Sutherland, D., Scales, S. J., Gould, S. E., Yauch, R. L., & deSauvage, F. J. (2011). Small molecule inhibition of GDC-0449 refractory smoothed mutants and downstream mechanisms of drug resistance. *Cancer Research*, 71, 435–444. <https://doi.org/10.1158/0008-5472.CAN-10-2876>
- Domenech, M., Bjerregaard, R., Bushman, W., & Beebe, D. J. (2012). Hedgehog signaling in myofibroblasts directly promotes prostate tumor cell growth. *Integrative Biology*, 4, 142–152. <https://doi.org/10.1039/c1ib00104c>
- Galperin, I., Dempwolff, L., Diederich, W. E., & Lauth, M. (2019). Inhibiting hedgehog: An update on pharmacological compounds and targeting strategies. *Journal of Medicinal Chemistry*, 62, 8392–8411. <https://doi.org/10.1021/acs.jmedchem.9b00188>
- Ghirga, F., Mori, M., & Infante, P. (2018). Current trends in hedgehog signaling pathway inhibition by small molecules. *Bioorganic & Medicinal Chemistry Letters*, 28, 3131–3140. <https://doi.org/10.1016/j.bmcl.2018.08.033>
- Lindsley, C. W. (2016). Novel drug approvals in 2015 and thus far in 2016. *ACS Chemical Neuroscience*, 7, 1175–1176. <https://doi.org/10.1021/acschemneuro.6b00254>
- Makley, L. N., & Gestwicki, J. E. (2013). Expanding the Number of ‘Druggable’ Targets: Non-Enzymes and Protein-Protein Interactions. *Chemical Biology & Drug Design*, 81, 22–32. <https://doi.org/10.1111/cbdd.12066>
- Mas, C., & Altaba, A. R. (2010). Small molecule modulation of hh-gli signaling: Current leads, trials and tribulations. *Biochemical Pharmacology*, 80, 712–723. <https://doi.org/10.1016/j.bcp.2010.04.016>
- Mathew, E., Zhang, Y. Q., Holtz, A. M., Kane, K. T., Song, J. Y., Allen, B. L., & diMagliano, M. P. (2014). Dosage-dependent regulation of pancreatic cancer growth and angiogenesis by hedgehog signaling. *Cell Reports*, 9, 484–494. <https://doi.org/10.1016/j.celrep.2014.09.010>
- Munchhof, M. J., Li, Q. F., Shavnya, A., Borzillo, G. V., Boyden, T. L., Jones, C. S., LaGreca, S. D., Martinez-Alsina, L., Patel, N., Pelletier, K., Reiter, L. A., Robbins, M. D., & Tkalcovic, G. T. (2012). Discovery of PF-04449913, a potent and orally bioavailable inhibitor of smoothed. *ACS Medicinal Chemistry Letters*, 3, 106–111. <https://doi.org/10.1021/ml2002423>
- Owens, A. E., dePaola, I., Hansen, W. A., Liu, Y. W., Khare, S. D., & Fasan, R. (2017). Design and evolution of a macrocyclic peptide inhibitor of the sonic hedgehog/patched interaction. *Journal of the American Chemical Society*, 139, 12559–12568. <https://doi.org/10.1021/jacs.7b06087>
- Pan, S. F., Wu, X., Jiang, J. Q., Gao, W. Q., Wan, Y. Q., Cheng, D., Han, D., Liu, J., Englund, N. P., Wang, Y., Peukert, S., Miller-Moslin, K., Yuan, J., Guo, R. B., Matsumoto, M., Vattay, A., Jiang, Y., Tsao, J., Sun, F. X., ... Dorsch, M. (2010). Discovery of NVP-LDE225, a potent and selective smoothed antagonist. *ACS Medicinal Chemistry Letters*, 1, 130–134. <https://doi.org/10.1021/ml1000307>
- Petrov, K. G., Zhang, Y. M., Carter, M., Cockerill, G. S., Dickerson, S., Gauthier, C. A., Guo, Y., Mook, R. A., Rusnak, D. W., Walker, A. L., Wood, E. R., & Lackey, K. E. (2006). Optimization and SAR for dual ErbB-1/ErbB-2 tyrosine kinase inhibition in the 6-furanylquinazoline series. *Bioorganic & Medicinal Chemistry Letters*, 16, 4686–4691. <https://doi.org/10.1016/j.bmcl.2006.05.090>
- Pricl, S., Cortelazzi, B., DalCol, V., Marson, D., Laurini, E., Fermeglia, M., Licitra, L., Pilotti, S., Bossi, P., & Perrone, F. (2015). Smoothed (SMO) receptor mutations dictate resistance to vismodegib in basal cell carcinoma. *Molecular Oncology*, 9, 389–397. <https://doi.org/10.1016/j.molonc.2014.09.003>
- Robarge, K. D., Brunton, S. A., Castanedo, G. M., Cui, Y., Dina, M. S., Goldsmith, R., Gould, S. E., Guichert, O., Gunzner, J. L., Halladay, J., Jia, W., Khojasteh, C., Koehler, M. F. T., Kotkow, K., La, H., LaLonde, R. L., Lau, K., Lee, L., Marshall, D., ... Xie, M. L. (2009). GDC-0449—A potent inhibitor of the hedgehog pathway. *Bioorganic & Medicinal Chemistry Letters*, 19, 5576–5581. <https://doi.org/10.1016/j.bmcl.2009.08.049>
- Romer, J. T., Kimura, H., Magdalena, S., Sasai, K., Fuller, C., Baines, H., Connelly, M., Stewart, C. F., Gould, S., Rubin, L. L., & Curran, T. (2004). Suppression of the Shh pathway using a small molecule inhibitor eliminates medulloblastoma in Ptc1^{+/-} p53^{-/-} mice. *Cancer Cell*, 6, 229–240. <https://doi.org/10.1016/j.ccr.2004.08.019>
- Salaritabar, A., Berindan-Neagoe, I., Darvish, B., Hadjiakhoondi, F., Manayi, A., Devi, K. P., Barreca, D., Orhan, I. E., Suntar, I., Farooqi, A. A., Gulei, D., Nabavi, S. F., Sureda, A., Daglia, M., Dehpour, A. R., Nabavi, S. M., & Shirooie, S. (2019). Targeting hedgehog signaling pathway: Paving the road for cancer therapy. *Pharmacological Research*, 141, 466–480. <https://doi.org/10.1016/j.phrs.2019.01.014>
- Sharpe, H. J., Wang, W. R., Hannoush, R. N., & deSauvage, F. J. (2015). Regulation of the oncoprotein smoothed by small molecules. *Nature Chemical Biology*, 11, 246–255. <https://doi.org/10.1038/nchembio.1776>
- Sheridan, M. H. (2019). Glasdegib: First global approval. *Drugs*, 79, 207–213. <https://doi.org/10.1007/s40265-018-1047-7>
- Trinh, T. N., McLaughlin, E. A., Gordon, C. P., & McCluskey, A. (2014). Hedgehog signalling pathway inhibitors as cancer suppressing

- agents. *Med Chem Commun*, 5, 117–133. <https://doi.org/10.1039/c3md00334e>
- Vesci, L., Milazzo, F. M., Stasi, M. A., Pace, S., Manera, F., Tallarico, C., Cini, E., Petricci, E., Manetti, F., DeSantis, R., & Giannini, G. (2018). Hedgehog pathway inhibitors of the acylthiourea and acylguanidine class show antitumor activity on colon cancer in vitro and in vivo. *European Journal of Medicinal Chemistry*, 157, 368–379. <https://doi.org/10.1016/j.ejmech.2018.07.053>
- Wahid, M., Jawed, A., Mandal, R. K., Dar, S. A., Khan, S., Akhter, N., & Haque, S. (2016). Vismodegib, itraconazole and sonidegib as hedgehog pathway inhibitors and their relative competencies in the treatment of basal cell carcinomas. *Critical Reviews in Oncology Hematology*, 98, 235–241. <https://doi.org/10.1016/j.critrevonc.2015.11.006>
- Yauch, R. L., Dijkgraaf, G. J., Aliche, B., Januario, T., Ahn, C. P., Holcomb, T., Pujara, K., Stinson, J., Callahan, C. A., Tang, T., Bazan, J. F., Kan, Z., Seshagiri, S., Hann, C. L., Gould, S. E., Low, J. A., Rudin, C. M., & deSavauge, F. J. (2009). Smoothed

mutation confers resistance to a hedgehog pathway inhibitor in medulloblastoma. *Science*, 326, 572–574. <https://doi.org/10.1126/science.1179386>

SUPPORTING INFORMATION

Additional supporting information may be found online in the Supporting Information section.

How to cite this article: Sun C, Zhang Y, Wang H, et al. Design and biological evaluation of phenyl imidazole analogs as hedgehog signaling pathway inhibitors. *Chem. Biol. Drug Des.* 2021;97:546–552. <https://doi.org/10.1111/cbdd.13799>